Talanta Open 2 (2020) 100013

Contents lists available at ScienceDirect

Talanta Open

journal homepage: www.elsevier.com/locate/talo

Ambient PM particles reach mouse brain, generate ultrastructural hallmarks of neuroinflammation, and stimulate amyloid deposition, tangles, and plaque formation

Saira Hameed, PhD[a], Jinzhuo Zhao, PhD[b,*], Richard N. Zare, PhD[a,*]

[a] Department of Chemistry, Fudan University, Shanghai 200438, China
[b] Department of Environmental Health, School of Public Health and the Key Laboratory of Public Health Safety, Ministry of Education, Fudan University, Shanghai 200032, China

ARTICLE INFO

Keywords:
Mouse brain
Particulate matter
Desorption electrospray ionization mass spectrometry imaging
Antibody staining
Fluorescence microscopy

ABSTRACT

Mice were exposed to ambient PM particles 8 h per day, 6 days per week, for twenty-four weeks in enrichment chambers, with real-time mass concentration of $PM_{2.5}$ around 70 μg/m^3, and the number of $PM_{0.1}$ about 10,000-20,000/m^3. The component analysis of PM particles by inductive coupled plasma emission spectrometer detected low concentrations of species associated with crustal materials, metalloid, transition metals, and heavy metals originating from industrial emission. High-performance liquid chromatography (HPLC) detected 22 polycyclic aromatic hydrocarbons originating from traffic exhausts. We found that PM particles from dirty air entered mouse brain which were visualized by field emission scanning electron microscopy (FE-SEM) and were counted by femtosecond pulsed laser illumination microscopy. FE-SEM of brain tissues from dirty air (n=8), and filtered air (control) (n=8) revealed ultrastructural hallmarks of neuroinflammation, enlarged perivascular space, and the attachment of inflammatory cells to the endothelium of blood vessels in brain. Exposure to dirty air containing ambient PM particles resulted in amyloid deposits and formation of neurofibrillary tangles and plaques. Desorption electrospray ionization mass spectrometry imaging enabled label-free elucidation of the spatial distribution of metabolites and lipids in brain tissue samples without any pretreatment. Ceramide Cer(t18:0/34:0(34OH)), *m/z* 822.54, and sulfatides, ST18:0, *m/z* 806.54; ST(d18:1/h22:0), *m/z* 878.60; ST(24:1), *m/z* 888.62, and ST(d18:1/h24:0), *m/z* 906.62 showed upregulation with significant differences in brain tissue from mice exposed to dirty air as compared to filtered air (control). The upregulation of ceramide resulted in formation of neurofibrillary tangles and plaques. Moreover, upregulation of sulfatides might enhance the leakiness of the blood brain barrier by weakening myelin sheaths. Although limited by sample number, our results strongly suggest that prolonged exposure to dirty air contributes to the observed increase in the incidence of cognitive decline and dementia, such as Alzheimer's disease.

Introduction

Uncontrolled wildfires, poor practices of agricultural waste management, rapid urbanization, traffic exhausts, and byproducts of the industrial revolution are generating airborne particulate matter (PM). According to the World Health Organization [46], air pollution kills an estimated seven million people worldwide each year, largely from increased mortality caused by stroke, heart disease, chronic obstructive pulmonary disease, lung cancer, and acute respiratory infections. Much less appreciated is the deleterious consequences of air pollution on the central nervous system [1]. Recently, Peeples has raised the alarm about this menace, which is pervasive in urban settings [37]. Numerous studies have reported that ambient PM, especially with an aerodynamic diameter less than 2.5 μm, named $PM_{2.5,}$ is associated with various adverse effects. Previous evidence showed that tiny PM is directly released into the air that can reach the brain [34]. The brain contains innate immune cells, such as microglia, that can respond to insult and injury via inflammation [4]. Therefore, based on the complex physiochemical nature of PM particles it has been hypothesized that once inside, they may act as inflammatory stimuli to activate innate immunity of brain cells contributing to pathology [5]. A previous study has found that cumulative $PM_{2.5}$ was significant for developing neurofibrillary tangles stage V in metropolitan Mexico City infants, which might be associated with the earliest cognitive and behavioral manifestations of Alzheimer's disease [8]. In the present study, mice were exposed to dirty air ($PM_{2.5}$) for six months to evaluate the consequences of air pollution on brain. Field

* Corresponding authors.
E-mail addresses: saira@fudan.edu.cn (S. Hameed), jinzhuozhao@fudan.edu.cn (J. Zhao), zare@stanford.edu (R.N. Zare).

https://doi.org/10.1016/j.talo.2020.100013
Received 24 July 2020; Received in revised form 31 August 2020; Accepted 31 August 2020

emission scanning electron microscopy (FE-SEM) was used to detect PM and examine signs of inflammation in mouse brain.

Neuroinflammation and brain damage are associated with a wide range of biochemical processes involving changes in the expression of metabolites and lipids [11, 23, 31]. Analysis of metabolites and lipids in brain tissue sections would provide a basis for further understanding of molecular mechanisms during neuropathological events [16]. For this purpose, we applied desorption electrospray ionization mass spectrometry imaging (DESI-MSI) that enables label-free elucidation of the spatial distribution of metabolites and lipids in biological tissue sections at ambient conditions without any pretreatment [2]. However, DESI-MSI does have a limitation of low spatial resolution which was overcome to some extent by fluorescent labeling. This methodology combined the unique advantages of DESI for biomolecular imaging, allowed the explicit matching of morphological and chemical features. An important advantage of the technique is that it preserves morphology of the analyzed samples for subsequent molecular and histopathology observations [14]. The data revealed high throughput detection of metabolites and lipids and allowed us to interpret the toxic effects of PM particles on brain that stimulated neuro-inflammation and developed neurofibrillary tangles and plaques. We were only able to harvest brain tissue from eight mice exposed for six months to dirty air and eight mice exposed for the same time period to filtered air (control). Brain samples were subsequently sliced into several thin sections and placed on glass slides for multiple analyses using FE-SEM, DESI-MSI, hematoxylin and eosin (H&E), and Congo red staining as well as antibody labeling. Femtosecond pulsed laser illumination microscopy was used to count the PM particles.

Materials and methods

Animal management

Six weeks old *Mus musculus* (C57BL/6 male mice) were purchased from Shanghai Jiesijie Laboratory Animal Co., Ltd (Shanghai, China). They were housed in a pathogen-free animal facility at Fudan University, at constant temperature (21°C ± 1°C) and humidity (60%) on a day and night cycle of 12 hours each, and were maintained on normal chow diet. The procedures were approved by the Institutional Research Committees of the Fudan University, Shanghai, China, and the methods were performed in accordance with the set regulations and guidelines. The numbers of mice were limited. We obtained eight brain samples from each group, after dirty air and filtered air exposure for six months. We prepared numerous thin sections for histopathology, FE-SEM, and DESI-MSI analyses.

Exposure of atmospheric particulate matter (PM) to mice

Mice were divided into two groups and were exposed to concentrated $PM_{2.5}$ (dirty air), and filtered air (control), using the "Shanghai Meteorological and Environmental Animal Exposure System (Shanghai-METAS)", located in the School of Public Health at Fudan University at Xujiahui District in Shanghai. We have used the exposure system to perform several studies [12, 13]. In this study, the exposure lasted for 8 h per day, 6 days per week, in a total of 24 weeks. The mice were freely allowed to eat food and drink water.

The real-time concentration of PM particles

The real-time concentrations of $PM_{2.5}$ were continuously measured by TEOM (Thermo Fisher Scientific, Waltham, MA), which was connected with the air intake in both exposure chamber and control chamber. The TEOM simultaneously sampled the $PM_{2.5}$ on Teflon filters (Gelman Teflon, 37 mm, 0.2 mm pore) for subsequent measuring the accurate concentrations and the components such as constituents of polycyclic aromatic hydrocarbons (PAHs) and trace metals.

Component analysis of PM particles

The Teflon filter (Gelman Teflon, 37 mm, 0.2 mm pore) with $PM_{2.5}$ was cut and divided into two parts. One part of filter was treated with 0.5 g potassium hydroxide. The other part of filter was treated with 10 mL of 60% high-purity nitric acid (HNO_3) and 3 mL of 37% perchloric acid ($HClO_4$). The solutions containing filters were heated in microwave for 1 h. They were then stored at 4°C until analysis. The metal concentrations of PM particles were determined using an Inductive Coupled Plasma Emission Spectrometer (Atom Scan 2000, Jarrell-Ash, USA), and the concentrations of polyaromatic hydrocarbons were determined by HPLC. For HPLC, samples were eluted from filters with 20 mL dichloromethane, filtered, dried under nitrogen atmosphere, and were then dissolved in methanol.

Preparation of brain tissue sections

The approval of the institutional review board was followed, the mice were sacrificed, and brain samples were collected and immediately stored at -80°C until sectioning. The samples were attached to the aluminum disc with a tiny drop of mounting medium at the bottom, and 10-μm-thick tissue slices were prepared using Leica CM1950 cryostat machine (Leica Biosystems), and were attached over the surface of adhesion microscopic glass slides (Shanghai Titan Scientific, Co., Ltd), and were stored in airtight falcon tubes of 50 mL capacity, containing silica gel beads at the bottom covered with a piece of tissue paper, to absorb residual moisture, and were stored at -80°C before analyses.

Field emission scanning electron microscopy (FE-SEM)

The falcon tubes containing glass slides of brain cryo-sections were kept at room temperature and dried before analysis without any pretreatment. The surface of the FE-SEM aluminum sample stage was covered with carbon conducting tape and the glass slide was attached onto it. Hitachi S-4800 field emission scanning electron microscope (FE-SEM) equipped with Bruker Xflash 6160 detector was used for observation of brain tissue sections of eight mice from dirty air and eight mice from filtered air, at acceleration voltage of 1.0 kV, and emission current of 10 μA. The vacuum level in the observation chamber was $\sim 10^{-7}$ Pa. The observations were made at the working distance of 2.1 mm to 2.4 mm, and at the scan speed of 20 seconds for each figure, at 10k, 20k, 50k, and 100k magnifications.

Femtosecond pulsed laser illumination microscopy

Teflon filters connected at the air inlet of TEOM 1405 (Thermo, USA) were separated, suspended in 0.9% physiological saline, sonicated for 30 min (Sonicator Model JL-120DT, China), and freeze-dried to collect $PM_{2.5}$ particles, that were observed using a Leica TCS SP8 DIVE FALCON microscope (Leica Germany) equipped with a two-photon femtosecond pulsed laser (810 nm, 150 fs, 80 MHz, InSight X3 Dual, USA) and a 10 × /0.4 objective. The second harmonic generation (SHG) signals from the $PM_{2.5}$ suspension were collected by a 400–410 nm BP filter. Each figure had a field of 1.16 mm x 1.16 mm, with 1024 × 1024 pixels. Signals were collected at a depth of 1 μm. Using the same method, the PM particles were counted from mouse brain tissues of three mice from dirty air and three mice from filtered air. The fluorescence of brain tissues was observed through a 450–610 nm bandpass filter.

Histological and immunohistochemical staining

The brain tissues were subjected to Hematoxylin & Eosin (H&E) and Congo red staining for histological evaluation. Staining was performed on the same mouse brain tissue sections after DESI-MSI, as well as on serial sections to visualize tissue morphological information. The H&E staining kit was obtained from Solarbio Life Sciences (Cat# G1120),

and Congo red dye was obtained from Ruibao and Biotech Co., Ltd (Cat# R1029). For immunohistochemical analyses the following antibodies and materials were used: IBA-1 (Reego and Biology, 1:100), Aβ (Reego and Biology, 1:500). HRP-labelled goat anti-rabbit secondary antibody (Reego and Biology, 1:200), DAB (DAKO, K5007), normal rabbit serum (Boster, AR1010), and BSA (Solarbio, A8020).

High resolution optical images of the stained tissues were observed by Olympus CKX53 microscope and recorded by using Olympus cellSens 2.1 [ver.2.1] imaging software for Life Sciences (Olympus, Tokyo, Japan).

Desorption electrospray ionization mass spectrometry imaging (DESI-MSI)

The DESI-MSI source controlled by the software OmniSpray 2-D (Prosolia, Inc.) coupled with Velos Pro Ion Trap Mass Spectrometer (Thermo Scientific, USA) was used for tissue imaging. The imaging experiments were performed under the same conditions. The precision cleaved emitter 50 μm ID x 150 μm OD x 40 mm long was used to make the spray head. The dimension of the solvent line tubing was 75 μm ID x 150 μm OD. The geometrical parameters were adjusted at a spray tip-to-surface distance ~1 mm, spray incident angle of 58°, and spray-to-inlet distance ~5 mm. MS Data acquisition was performed using XCalibur 2.2 software (Thermo Fisher Scientific Inc.). The nitrogen pressure was set at 1.02 MPa; spray voltage was 4 kV, capillary temperature of 275°C, S-Lens RF Level of 60.6%. The brain tissue samples were analyzed at the negative ion mode from m/z 150 to m/z 1000. The histology compatible solvent used for both ion modes was dimethylformamide/acetonitrile (DMF + ACN) (1:1, v/v) [14] obtained from Fisher Chemical NJ, at flow rate of 1 μL/min. The data files (.raw) were exported to FireFly 3 software (Prosolia, Inc.) that extracted and built the data set into (.ibd and .imzML) formats. msIQuant software was used to convert imzML data files to msiQuant readable format to view and analyze mass spectrometry imaging data [21]. The ion images used a Bruker rainbow color map to represent highest intensity by pink and the lowest intensity by black.

Statistical analysis

Owing to limited availability, mouse brains (n=8) from each group were used to obtain several thin sections of tissue for multiple analyses and evaluations. The differences in measured variables between dirty air and filtered air exposure groups were analyzed by independent-samples t test. A p-value ≤ 0.05 was defined as statistically significant.

Metabolite/Lipid identification

The molecular signals observed in the mass spectrometry data were identified and confirmed from previous reports summarized in review [3], and database search including LIPID Maps structural database (LMSD) (http://lipidmaps.org/data/structure/LMSDSearch.php?Mode=SetupTextOntologySearch), and Human Metabolome Database (HMDB) search engines (http://www.hmdb.ca/spectra/ms/search).

Results

Air quality data

Sixteen mice were divided equally into dirty air and filtered air (control) groups, and they were housed in the Shanghai Meteorological and Environmental Animal Exposure System (Shanghai-METAS), located in the School of Public Health at Fudan University at Xujiahui District in Shanghai. Shanghai-METAS captured $PM_{2.5}$ particles from ambient air and increased their concentration about two times higher than that of ambient air in the metropolitan area for the year 2019. The real-time concentrations of $PM_{2.5}$ were continuously measured by TEOM 1450 (Thermo Fisher Scientific, Waltham, MA), which was connected with the air intake in both dirty air and filtered air (control) chambers. Some variations in concentration depending on traffic flow and weather changes during six months of exposure were observed because the ambient air from the metropolitan area was the direct source of $PM_{2.5}$ particles that were collected in the exposure chamber. The concentration of PM particles from the air samples monitored over six months of exposure is shown in Fig. S1. The mass concentration of $PM_{2.5}$ was around 70 $\mu g/m^3$, and the number of $PM_{0.1}$ was around 10000-20000/m^3. The TEOM simultaneously sampled $PM_{2.5}$ on Teflon filters (Gelman Teflon, 37 mm, 0.2 mm pore), for subsequent measurement of accurate concentrations and components analysis.

Concentrations of metals were determined using an Inductive Coupled Plasma Emission Spectrometer (Atom Scan 2000, Jarrell-Ash, USA). Low concentrations of metals (Na, K, Mg, Ca, Sr, Ba, Al) associated with crustal material, transition metals (Ti,Cr, Mn, Fe, Cu, Zn), metalloid (As), and heavy metal (Pb) were detected. They are believed to originate from industrial emissions. High performance liquid chromatography (HPLC) was used that detected PAHs (fluorine, phenanthrene, anthracene, fluoranthene, acephenanthrene, pyrene, retene, benzo[g,h,i]fluoranthene, cyclopenta[cd]pyrene, benz[a]anthracene, benzo[b]fluoranthene, benzo[k]fluoranthene, benzo[a]fluoranthene, benzo[e]pyrene, benzo[a]pyrene, perylene, 1,3,5-triphenylbenzene, indo[cd]fluoranthene, indeno[cd] pyrene, dibenzo[ah]anthracene, benzo[ghi]perylene, and coronene) that are believed to originate from traffic exhausts. Table S1 summarizes the results of the component analysis.

PM particles from air pollution reached mouse brain

Fig. 1A presents a graphical illustration showing the movement of PM particles inside the respiratory track while breathing. During respiration, the PM particles of different sizes and shapes enter the respiratory track and attach onto the surfaces of nasal epithelial cells. The respiratory track is lined with cilia that are always in the state of motion which creates mucus flow [22]. The strokes of cilia propel fine particles coated with mucus in a unidirectional flow [40]. PM particles from dirty air translocate into brain (Fig. 1B), and from the nasal epithelial mucosa enters into the brain via the olfactory bulb in mouse [34], and human [28]. PM moves in the blood capillary lining of brain cells (Fig. 1C). Interestingly, ultrafine particles enter into the blood circulation of humans just after exposure [33], and have the potency to reach various organ systems.

FE-SEM of brain tissues from filtered air showed no particles (Fig. 1D). In sharp contrast, the brain tissues from dirty air (more specifically, 8 h per day, 6 days per week) showed different PM particles scattered over the surface (Figs. 1E-L).

PM particles on brain tissues were counted by femtosecond pulsed laser illumination microscopy, and Fig. 2 presents the results. Each panel had a field of 1.16 mm x 1.16 mm with 1024 × 1024 pixels, and the signal was collected within the depth of about 1 μm. Brain tissues from filtered air showed few to almost no particles (Fig. 2A), whereas mouse brain tissues from dirty air showed PM particles that emitted red light under femtosecond pulsed light illumination (Fig. 2B), and particles were quantified from three slides (Fig. 2C). The average number of particles detected on the brain tissue surface from filtered air were 867, and brain tissue from dirty air were 4458.

We also tried scanning electron microscopy / energy dispersive X-Ray spectroscopy (**SEM/EDS**) to perform elemental/ component analysis of PM particles in brain tissue sections, but it was not successful because the PM particles were scattered over brain tissue sections as tiny particles in nm size range, and no big cluster was found.

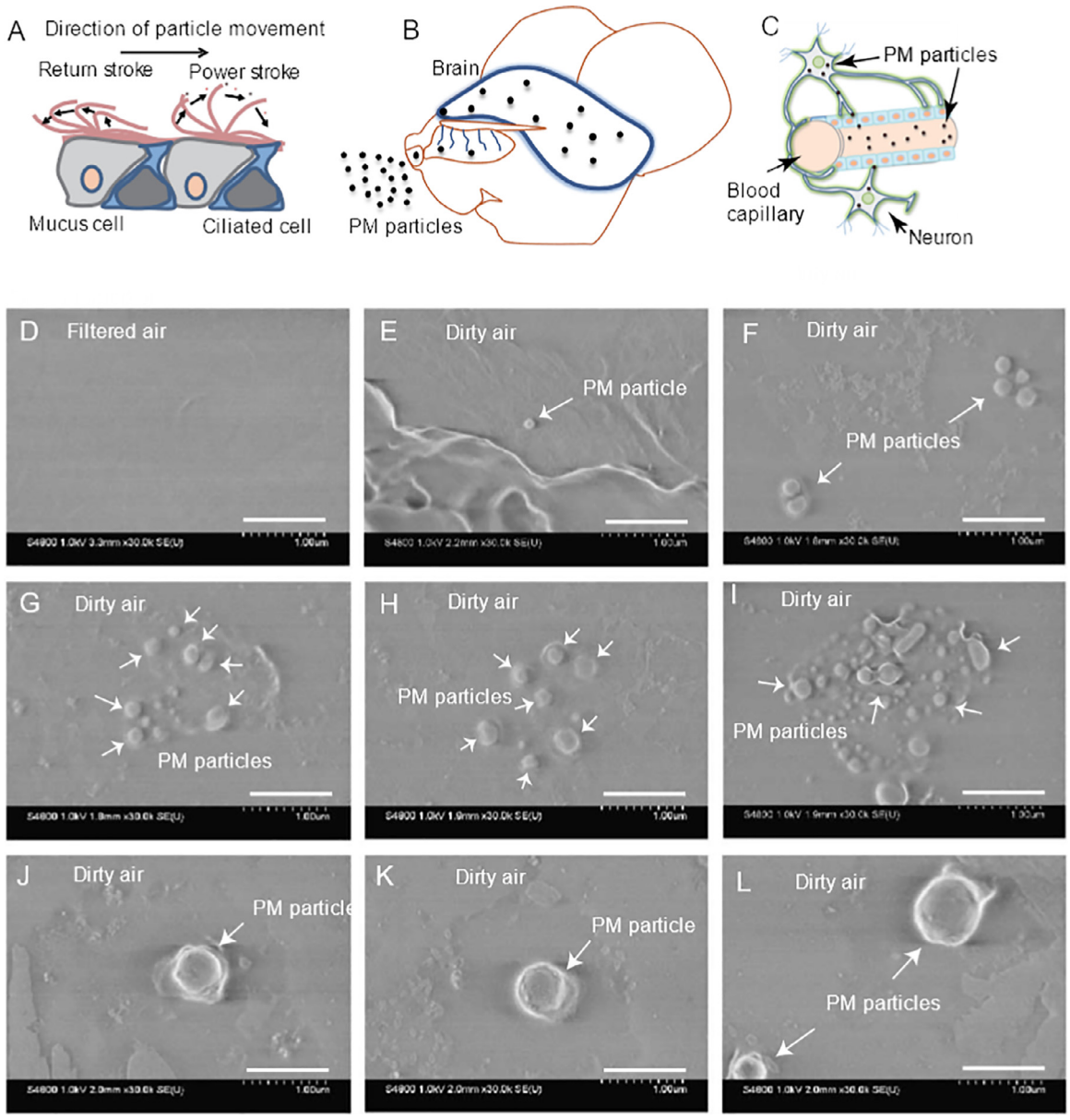

Fig. 1. Particulate matter (PM) from dirty air entered mouse brain. (**A**) Graphical illustration of the movement of particles inside the respiratory track during breathing; (**B**) Translocation of PM particles into brain through olfactory neurons inside mouse nose; and (**C**) Movement of PM particles in the blood capillary lining brain cells. (**D**) Surface evaluation of mouse brain tissues by FE-SEM in which brain tissue from filtered air showed no abnormality, whereas (**E-L**) brain tissue from dirty air showed different PM particles scattered over the surface (n=8). The scale bar at 30k magnification (**D-L**) is 1 μm.

Exposure of particulate matter from dirty air to brain generated ultrastructural hallmarks of neuroinflammation

FE-SEM of brain tissues from filtered air showed no abnormality (Fig. 3A), whereas brain tissues from dirty air showed inflammatory cells attached with the endothelium layer of blood vessels in the brain (Fig. 3B) and enlarged perivascular space (Fig. 3C). We also found anatomical changes and prominent topological alterations that suggested neuroinflammation on the brain surface (Fig. 3D-3I).

Histopathological evaluation revealed neurofibrillary tangles, plaques, and amyloid deposition in brain

We used hematoxylin & eosin (H&E), Congo red staining, and immunohistochemistry with Aβ and IBA-1 antibodies to check the toxic effects of particulate matter exposure on neuromorphology. H&E stained mouse brain tissues from the filtered air showed no abnormalities (Fig. 4A), as compared to the dirty air that showed neurofibrillary tangles and plaques (Fig. 4B–4D). Congo red stained mouse brain tissue from filtered air showed no abnormalities (Fig. 4E), as compared to the dirty air that showed accumulation of inflammatory glia cells (Fig. 4F), and amyloid deposits (Fig. 4G–4J). Immunohistochemistry with Aβ antibody showed amyloid deposits in the brain tissues from dirty air (Fig. 4K–4N). Immunohistochemistry with IBA-1 antibody showed accumulation of inflammatory glia cells in the brain tissues from dirty air (Fig. 4O–4R).

Metabolic alterations in mouse brain characteristic of neurodegeneration

Desorption electrospray ionization (DESI) mass spectrometry imaging (MSI) is an efficient diagnostic and research tool. The results of mouse brain sections used for DESI-MSI and for subsequent FE-SEM and

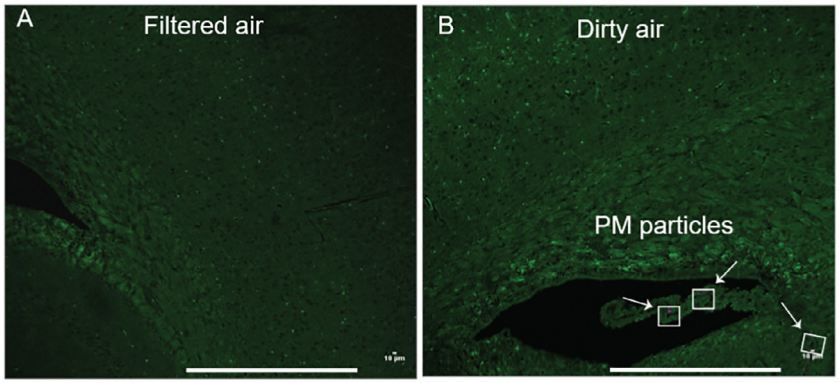

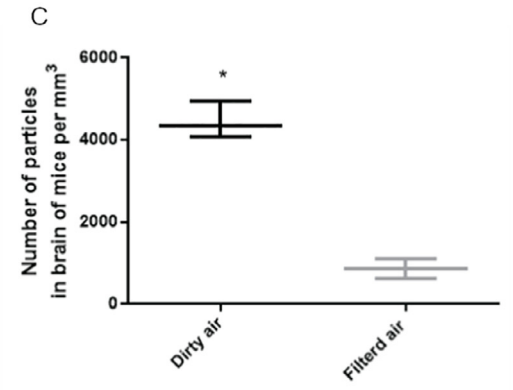

Fig. 2. PM particles on brain tissues were counted by femtosecond pulsed laser illumination microscopy analyses. (**A**) Mouse brain tissues from filtered air showed no particles, and two-photon excited autofluorescence from brain (green, emission (450-610 nm bandpass filter) was observed, whereas (**B**) mouse brain tissues from dirty air emitted red light originating from the PM particles (indicated using white squares), under femtosecond pulsed laser illumination (excitation 810 nm, 80 MHz, 10 mW laser power). Scale bar (**A**-**B**) is 400 μm. (**C**) Quantitative count of PM particles from mouse brain tissues of filtered air and dirty air groups reported as the mean ± one standard deviation (SD) (n=3). The *p* values (p=0.000261) were calculated using the *t* test.

histopathological evaluations were compared with results from independent analysis of mouse brain tissue serial sections that showed no difference.

Metabolic profiling of mouse brain samples from dirty air and filtered air exposure groups was performed by desorption electrospray ionization (DESI) mass spectrometry imaging (MSI) obtained at negative ion mode over the range of 150 *m/z* to 1000 *m/z*. The peaks in low mass range such as *m/z* 255.23 and *m/z* 283.26 were background peaks. The mass spectra from two groups with eight pairs of mice showed significant differences in the abundance of metabolites and lipids related to neurodegeneration (Fig. 5A and 5B), and is illustrated in 2D chemical maps (ion images) created using msIQuant software [21]. The data revealed detection of ceramide, Cer(t18:0/34:0(34OH)), *m/z* 822.54, and sulfatides, ST18:0, *m/z* 806.54; ST(d18:1/h22:0), *m/z* 878.60; ST(24:1), *m/z* 888.62, and ST(d18:1/h24:0), *m/z* 906.62. Table S2 summarizes information about the detected lipid molecular species from the mouse brain tissues, and Fig. S2 shows their structures.

Ceramide and sulfatides were upregulated with significant differences in brain tissue from dirty air (Fig. 5B upper panel) compared to the filtered air exposure groups (Fig. 5B lower panel). The data, presented as mean and ± one standard deviation (SD), are shown from 8 independent measurements of each group. The *p* values were calculated using independent-samples *t* test, for *m/z* 806.54 (p=0.0279), *m/z* 822.54 (p=0.0508), *m/z* 878.60 (p=0.0428), *m/z* 888.62 (p=0.022) and *m/z* 906.62 (p=0.0545) (Fig. 5C).

Discussion

Eight mice were exposed to ambient PM particles for twenty-four weeks in enrichment chambers with about two times higher concentration of PM particles than ambient air in the metropolitan area during 2019, which allows accelerated testing. An epidemiological study in China found an association between severe (332 μg/m^3 PM_{10}) air pollution and injury to the central nervous system, as measured by the number of medical emergency calls concerning dizziness, convulsions, paralysis, and epilepsy [10]. But little seems to be known about prolonged exposure to less severe air pollution. We had considered the damage of regular PM particle concentration and tried to make one group of mice exposure to normal air and another group of mice exposure to filtered air (FA). However, it needed long time exposure to find the difference of brain-related indicators between these two groups. In addition, because Shanghai is a relatively clean city in China, ambient $PM_{2.5}$ concentrations are very low most of time even similar with the concentration in the FA chamber. Therefore, it is difficult to observe the difference between regular air and filtered air.

For what we are calling dirty air, the real-time mass concentration of $PM_{2.5}$ was around 70 μg/m^3, and the number of $PM_{0.1}$ was around 10,000-20,000/m^3 (Fig. S1). The component analysis of PM particles by inductive coupled plasma emission spectrometer and HPLC detected low concentrations of metals associated with crustal materials, metalloid, transition and heavy metals that originated from industrial emissions, and 22 polycyclic aromatic hydrocarbons that originated from traffic exhausts (Table S1). We found that PM particles from dirty air entered into mouse brain, and these particles were visualized by FE-SEM (Fig. 1 E-L), and were counted by femtosecond pulsed laser illumination microscopy (Fig. 2). The components of PM particles act in different ways to cause brain damage [37]. A recent *in vivo* study reported that the placental barrier is permeable to carbon black particles from atmospheric pollution [6]. An epidemiological study from Mexico City found that Alzheimer's disease occurred in the brains of children [8]. However, the nervous system is protected by the semipermeable membrane of endothelial cells known as the blood brain barrier which controls and regulates the flow of essential molecules, oxygen, metabolites, and nutrients, into the brain through passive diffusion [24]. The brain capillaries

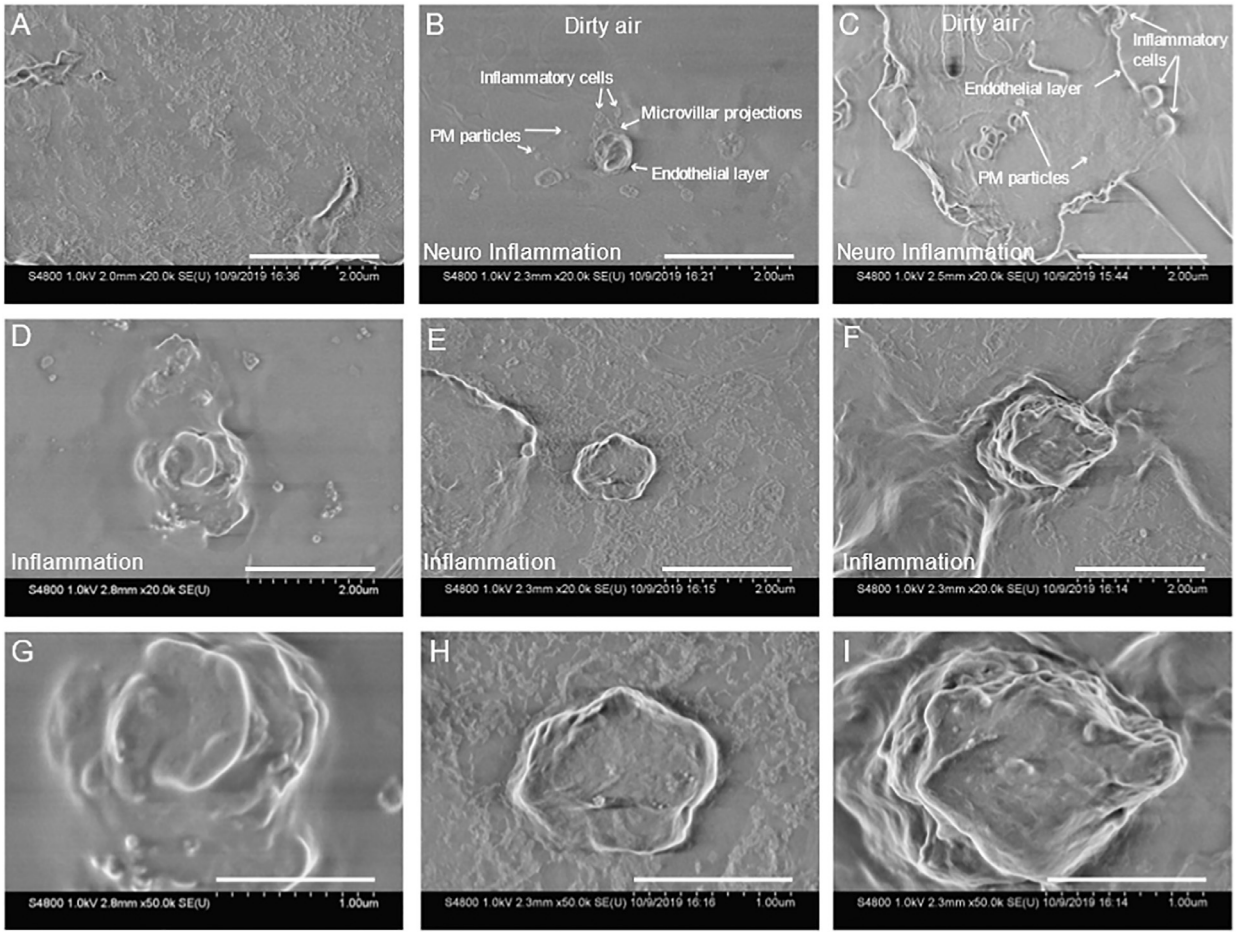

Fig. 3. Evaluation of topological features of mouse brain tissues by FE-SEM. (**A**) Mouse brain tissue from filtered air showed no abnormality. (**B**) Mouse brain tissue from dirty air showed features resembling inflammatory cells attaching with microvillar projections of endothelium of the blood vessel. (**C**) The exposure of particulate matter to brain activates the immune response and enlarged perivascular space. (**D-I**) Observation of anatomical features and topological alterations suggesting neuroinflammation. The scale bar at 20k magnification (**A -F**) is 2 μm, and at 50k magnification (**G-I**) is 1 μm.

are composed of tightly bound endothelial cells that restrict the entry of blood-derived cells into the brain, unless they have special surface properties that facilitate their transportation into the brain [42]. The disruption in the blood brain barrier results in increased vascular permeability, reduction of cerebral blood flow, and altered hemodynamic signals, which stimulates the influx of toxic substances from the blood into the brain and triggers inflammation and immune response. In turn, this stimulates pathways of neurodegeneration in different parts of the brain [42]. Previous study suggested that airborne PM accelerates neurodegenerative processes of Alzheimer's disease and related dementias through pro-amyloidogenic amyloid precursor protein processing [7]. Based on FE-SEM observations, morphological evidence of chronic inflammation at the brain blood vessels is revealed resulting from particulate matter exposure from dirty air (Fig. 3). Our observation is supported by previous studies that have shown that blood vessels from brain and spinal cord of mice subjected to experimental allergic encephalomyelitis and cerebral malaria in response to chronic inflammation showed attachment of inflammatory cells to the microvillar projections of the effected endothelium [25–27].

The plausible links between air quality and cognitive decline and dementia have been reviewed recently [38]. Previous studies have shown that particulate matter in air generates cognitive defects in older people, and causes inflammation in glial cells [7]. The brain of a mouse breathing dirty air produces inflammatory molecules, which are the same as found in Alzheimer's disease, and show nerve cell damage [48]. The data we present show neurofibrillary tangles and plaques in the mouse brain tissue sections from the dirty air (containing PM particles) exposure (Fig. 4), which is supported by previous reports that showed that Aβ peptides are deposited as a result of oxidative stress and neurofibrillary tangles are formed that serve as a shields to protect brain cells from the oxidative damage [32]. However, these evolve into an auto-destructive process as the disease progresses [31, 39].

What might make the present study of special interest is our direct observation of brain damage in mice on prolonged exposure to dirty air containing about two times higher concentration of PM particles than ambient air in the metropolitan area, and compared to filtered air (control). We have determined this to be the case from the observation of tangles and plaques in the brain (Fig. 4), and more indirect evidence by using DESI-MSI to show the buildup of certain compounds that are known to be associated with brain cell apoptosis (Fig. 5). The correlations presented seem compelling that some causal relation exists. Previous studies have shown that fatty acids are released at the site of brain injury and activate caspase-3 and caspase-8, which induces apoptosis [44]. The injury results in tissue damage, disturbance in ion balance, neurotransmitter release, and degradation of cellular phospholipids [45]. Moreover, free fatty acids interact with intracellular fatty acid binding proteins and peroxisome proliferator-activated receptors which leads to changes in gene expression [47]. DESI-MSI allowed the evaluation of the molecular events taking place in brain tissue samples caused by PM exposure, which activates immune response and development of disease state. The metabolites and lipids detected from the limited number of brains (eight from each group) hindered the ability

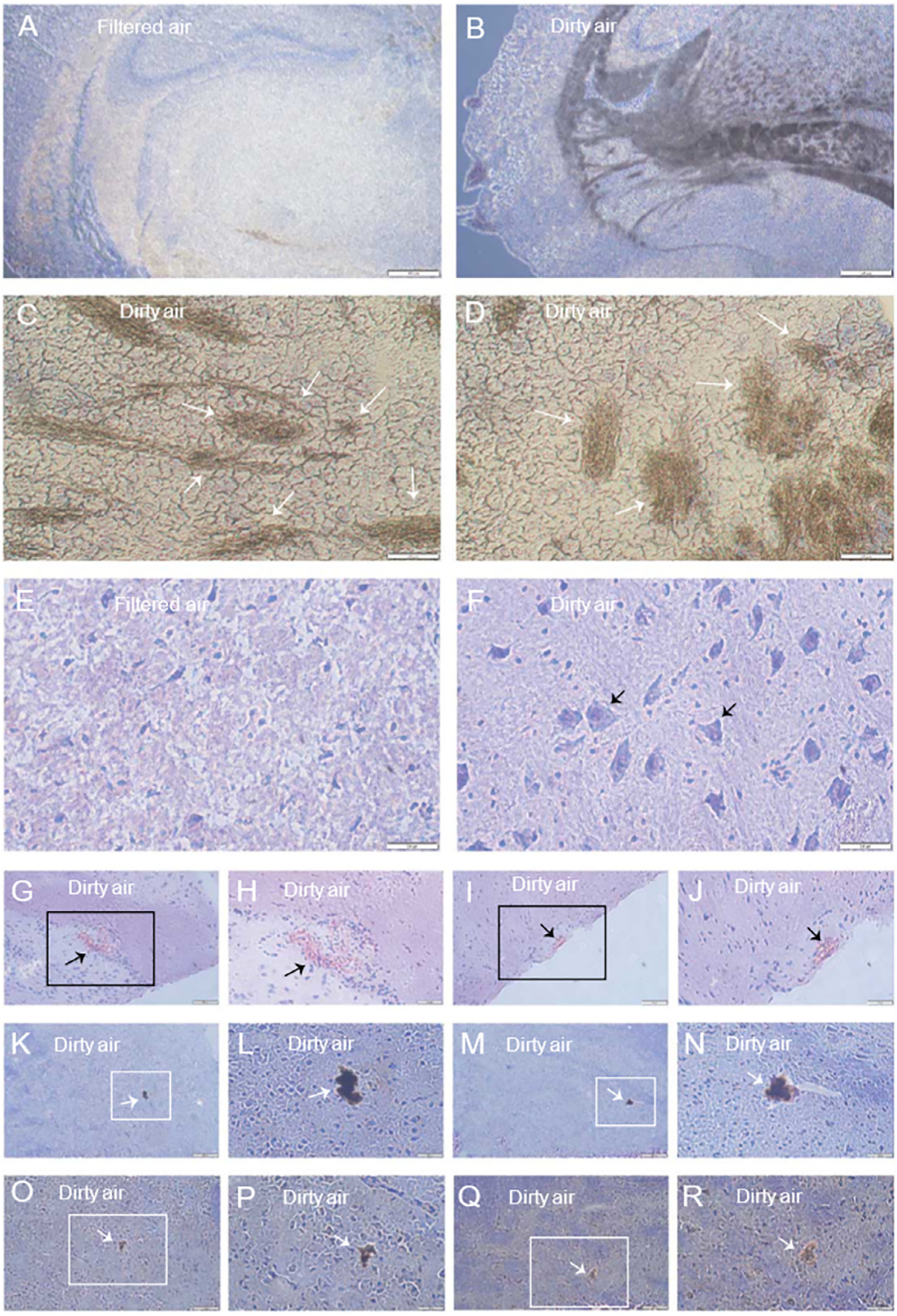

Fig. 4. Histopathological evaluations of mice brain tissues. (**A**) H&E stained mouse brain tissues from filtered air showed no abnormalities, whereas (**B-D**) mouse brain tissues from the dirty air showed neurofibrillary tangles and plaques. (**E**) Congo red stained mouse brain tissue from filtered air showed no abnormality, whereas (**F**) mouse brain tissues from dirty air showed accumulation of inflammatory glia cells, and (**G-J**) amyloid deposits. (**K-N**) Immunohistochemistry with Aβ antibody (1:500) of mouse brain from dirty air showed amyloid deposits. (**O-R**) Immunohistochemistry with IBA-1 antibody (1:100) of mouse brain tissues from dirty air showed accumulation of inflammatory glia cells. The scale bar at 4X magnification (**A-B**), 10X magnification (**K, M**), 20X magnification (**G, I, O, Q**), and 40X magnification (**C-F, H, J, L, N, P, R**) is 500 μm.

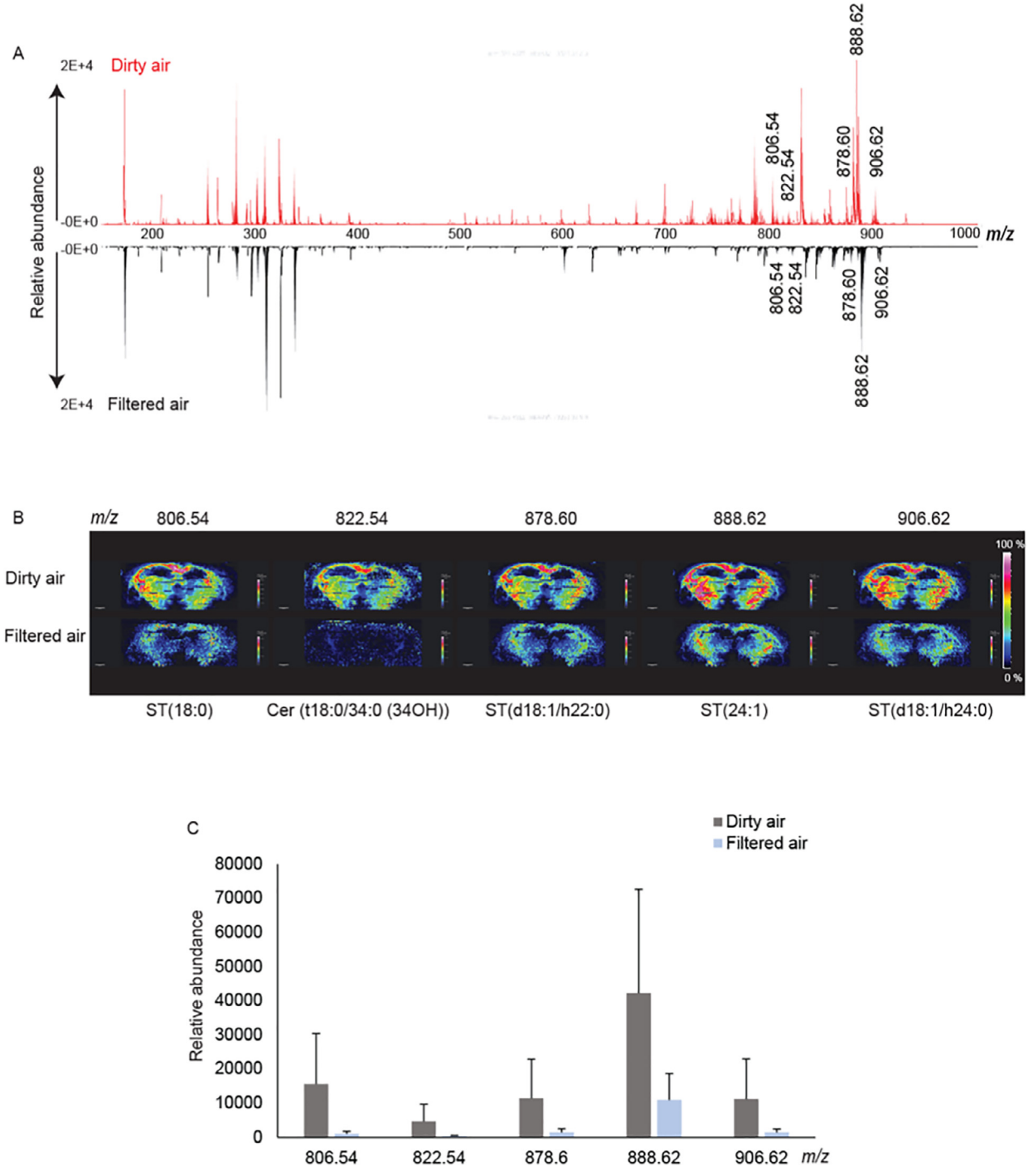

Fig. 5. Profiling of metabolic alterations in mouse brain. Mass spectra of brain samples from the exposure groups: (**A**) dirty air (red spectrum), and filtered air (control) (black spectrum). (**B**) Ion images of mouse brain (dirty air upper panel, filtered air lower panel), ST18:0, *m/z* 806.54; Cer(t18:0/34:0(34OH)), *m/z* 822.54; ST(d18:1/h22:0), *m/z* 878.60; ST(24:1), *m/z* 888.62, and ST(d18:1/h24:0), *m/z* 906.62. Rainbow color scale: black no signal and pink high intensity signal. Scale bar: 1 mm. (**C**) Quantitative signal intensities reported as the mean ± one standard deviation (SD) (n=8). The *p* values were calculated using the *t* test: *m/z* 806.54 (p=0.0279), *m/z* 822.54 (p=0.0508), *m/z* 878.60 (p=0.0428), *m/z* 888.62 (p=0.022) and *m/z* 906.62 (p=0.0545).

to detect statistically significant results as shown in Fig. 5. Nevertheless, we did find from brain tissues clear evidence for upregulation of ceramide, Cer(t18:0/34:0(34OH)), *m/z* 822.54in the brain tissues from the dirty air (Fig. 5B upper panel), as compared to the filtered air (control) (Fig. 5B lower panel). Ceramides play an important role in apoptosis [18], differentiation [35], and inflammation [30]. Previous studies have detected upregulation of ceramide molecules in injured rat brain [17]. Moreover, the studies showed that ceramide and brain damage co-localize, suggesting direct role of sphingomyelin metabolism in neuronal cell death [17]. Ceramide is the main product of sphingolipid metabolism, and it is directly involved in the aggregation of amyloid beta (Aβ) for the progression of Alzheimer's disease [20] through stabilization of the enzyme β-secretase. As a result of a positive feedback mechanism, the generated Aβ activates the sphingomyelinase enzyme that catabolizes sphingomyelin and increases ceramide levels in the brain [36]. Ceramide also activates a number of biochemical processes

leading to malfunctioning of mitochondria [41], and generation of oxidative stress through production of reactive oxygen species [9].

In addition, sulfated galactosyl ceramide also known as sulfatides (ST) that belong to glycosphingolipids [19], are found in abundance at the myelin sheath of brain cells [29]. We found upregulation of sulfatides, ST18:0, *m/z* 806.54; ST(d18:1/h22:0), *m/z* 878.60; ST(24:1), *m/z* 888.62, and ST(d18:1/h24:0), *m/z* 906.62 in the brain tissues from dirty air (Fig. 5B upper panel), as compared to the filtered air (Fig. 5B lower panel), suggesting damages in the myelin sheath and blood brain function dysfunction as a result of particulate matter exposure. This hypothesis is supported by previous reports that have shown that the expression levels of sulfatides are associated with the physiological activity of the blood brain barrier, and increased concentration of sulfatide has impact on myelin sheath at early stages of HIV-1 infection [15]. Moreover, abnormalities in the expression of sulfatides in brain result in neurological symptoms, because they regulate function of ion channels, receptors, and transporters [43].

Concluding remarks

Inhaling air containing particulate matter $PM_{2.5}$ is known to be deleterious to health, particularly to lung function, but this study presents striking visual evidence of its harmful effects on brain tissue. The component analysis of PM particles by inductive coupled plasma emission spectrometer and HPLC detected low concentrations of metals associated with crustal materials, metalloid, transition and heavy metals that originated from industrial emission, and 22 polycyclic aromatic hydrocarbons that originated from traffic exhausts. In conclusion, our study provides compelling evidence from FE-SEM and FLIM for the presence of PM particles in mouse brain, which originated from exposure of mice to atmospheric pollution. Moreover, the study shows systemic inflammation in response to accumulation of PM particles in the mouse brain. Eight mice were exposed to dirty air for six month and under the same feeding conditions another set of eight mice were exposed to filtered air. The present study found detrimental effects of this exposure that resulted in amyloid deposits, formation of tangles and plaques, and triggered inflammatory response in mouse brain. DESI-MSI revealed co-localized alterations in metabolic homeostasis of the mouse brain. Upregulation of ceramide, Cer(t18:0/34:0(34OH)), *m/z* 822.54 may generate reactive oxygen species that damage the brain. Moreover, upregulation of sulfatides, ST18:0, *m/z* 806.54; ST(d18:1/h22:0), *m/z* 878.60; ST(24:1), *m/z* 888.62, and ST(d18:1/h24:0), *m/z* 906.62 damages myelin sheath which can cause malfunctioning of the blood brain barrier. Our results must be taken in the context of a limited sample number of mice studied, but our findings strongly support the contention that prolonged exposure to $PM_{2.5}$ airborne pollutants increase the risk of cognitive decline and dementia.

Declaration of Competing Interest

The authors declare no competing interests.

CRediT authorship contribution statement

Saira Hameed: Visualization, Formal analysis, Writing - original draft. **Jinzhuo Zhao:** Writing - original draft, Conceptualization. **Richard N. Zare:** Visualization, Writing - original draft.

Acknowledgments

We are grateful to Hao Chen, Department of Chemistry, New Jersey Institute of Technology for useful comments and Cao Hui, Department of Material Sciences, Fudan University for assistance with FE-SEM. SH and RNZ thank the Scientific Research Startup Foundation (IDH1615113) of Fudan University for funding to make this study possible.

Supplementary materials

Supplementary material associated with this article can be found, in the online version, at doi:10.1016/j.talo.2020.100013.

References

[1] A.A. Almetwally, M. Bin-Jumah, A.A. Allam, Ambient air pollution and its influence on human health and welfare: an overview, Environ. Sci. Pollut. Res. 27 (2020) 24815–24830.
[2] S. Banerjee, R.N. Zare, R.J. Tibshirani, C.A. Kunder, R. Nolley, R. Fan, et al., Diagnosis of prostate cancer by desorption electrospray ionization mass spectrometric imaging of small metabolites and lipids, Proc. Natl. Acad. Sci. U. S. A. 114 (2017) 3334–3339.
[3] K.A. Berry, J.A. Hankin, R.M. Barkley, J.M. Spraggins, R.M. Caprioli, R.C. Murphy, Maldi imaging of lipid biochemistry in tissues by mass spectrometry, Chem. Rev. 111 (2011) 6491–6512.
[4] M.L. Block, L. Zecca, J.S. Hong, Microglia-mediated neurotoxicity: Uncovering the molecular mechanisms, Nat. Rev. Neurosci. 8 (2007) 57–69.
[5] M.L. Block, L. Calderon-Garciduenas, Air pollution: Mechanisms of neuroinflammation and CNS disease, Trends Neurosci. 32 (2009) 506–516.
[6] H. Bove, E. Bongaerts, E. Slenders, E.M. Bijnens, N.D. Saenen, W. Gyselaers, et al., Ambient black carbon particles reach the fetal side of human placenta, Nat. Commun. 10 (2019) 3866.
[7] M. Cacciottolo, X. Wang, I. Driscoll, N. Woodward, A. Saffari, J. Reyes, et al., Particulate air pollutants, apoe alleles and their contributions to cognitive impairment in older women and to amyloidogenesis in experimental models, Transl. Psychiatry 7 (2017) e1022.
[8] L. Calderon-Garciduenas, A. Gonzalez-Maciel, R. Reynoso-Robles, R. Delgado-Chavez, P.S. Mukherjee, R.J. Kulesza, et al., Hallmarks of Alzheimer disease are evolving relentlessly in metropolitan Mexico city infants, children and young adults. Apoe4 carriers have higher suicide risk and higher odds of reaching nft stage v at </=40 years of age, Environ. Res. 164 (2018) 475–487.
[9] S. Chakrabarti, M. Sinha, I.G. Thakurta, P. Banerjee, M. Chattopadhyay, Oxidative stress and amyloid beta toxicity in Alzheimer's disease: Intervention in a complex relationship by antioxidants, Curr. Med. Chem. 20 (2013) 4648–4664.
[10] L. Cui, G.A. Conway, L. Jin, J. Zhou, J. Zhang, X. Li, et al., Increase in medical emergency calls and calls for central nervous system symptoms during a severe air pollution event, January 2013, Jinan City, China, Epidemiol. (Camb. Mass) 28 (Suppl 1) (2017) S67–S73.
[11] G. Di Paolo, T.W. Kim, Linking lipids to Alzheimer's disease: cholesterol and beyond, Nat. Rev. Neurosci. 12 (2011) 284–296.
[12] X. Du, S. Jiang, X. Zeng, J. Zhang, K. Pan, J. Zhou, et al., Air pollution is associated with the development of atherosclerosis via the cooperation of cd36 and nlrp3 inflammasome in apoe(-/-) mice, Toxicol. Lett. 290 (2018) 123–132.
[13] X. Du, S. Jiang, X. Zeng, J. Zhang, K. Pan, L. Song, et al., Fine particulate matter-induced cardiovascular injury is associated with nlrp3 inflammasome activation in apo e(-/-) mice, Ecotoxicol. Environ. Saf. 174 (2019) 92–99.
[14] L.S. Eberlin, C.R. Ferreira, A.L. Dill, D.R. Ifa, L. Cheng, R.G. Cooks, Nondestructive, histologically compatible tissue imaging by desorption electrospray ionization mass spectrometry, ChemBioChem 12 (2011) 2129–2132.
[15] M. Gisslen, P. Fredman, G. Norkrans, L. Hagberg, Elevated cerebrospinal fluid sulfatide concentrations as a sign of increased metabolic turnover of myelin in HIV type I infection, AIDS Res. Hum. Retrovir. 12 (1996) 149–155.
[16] S. Hameed, Y. Sugiura, Y. Kimura, K.K. Shrivas, M. Setou, Nanoparticle-assisted laser desorption/ionization (nano-paldi)-based imaging mass spectrometry (ims) and its application to brain sciences, in: Nanomedicine and the Nervous System, CRC Press, 2012, pp. 97–118.
[17] J.A. Hankin, S.E. Farias, R.M. Barkley, K. Heidenreich, L.C. Frey, K. Hamazaki, et al., Maldi mass spectrometric imaging of lipids in rat brain injury models, J. Am. Soc. Mass Spectrom. 22 (2011) 1014–1021.
[18] Y.A. Hannun, L.M. Obeid, Ceramide: An intracellular signal for apoptosis, Trends Biochem. Sci. 20 (1995) 73–77.
[19] I. Ishizuka, Chemistry and functional distribution of sulfoglycolipids, Prog. Lipid Res. 36 (1997) 245–319.
[20] M. Jazvinscak Jembrek, P.R. Hof, G. Simic, Ceramides in Alzheimer's disease: Key mediators of neuronal apoptosis induced by oxidative stress and abeta accumulation, Oxid. Med. Cell. Longev. 2015 (2015) 346783.
[21] P. Kallback, A. Nilsson, M. Shariatgorji, P.E. Andren, Msiquant–quantitation software for mass spectrometry imaging enabling fast access, visualization, and analysis of large data sets, Anal. Chem. 88 (2016) 4346–4353.
[22] T.A. Katoh, K. Ikegami, N. Uchida, T. Iwase, D. Nakane, T. Masaike, et al., Three-dimensional tracking of microbeads attached to the tip of single isolated tracheal cilia beating under external load, Sci. Rep. 8 (2018) 15562.
[23] I. Kaya, H. Zetterberg, K. Blennow, J. Hanrieder, Shedding light on the molecular pathology of amyloid plaques in transgenic alzheimer's disease mice using multimodal maldi imaging mass spectrometry, ACS Chem. Neurosci. 9 (2018) 1802–1817.
[24] K. Kisler, A.R. Nelson, A. Montagne, B.V. Zlokovic, Cerebral blood flow regulation and neurovascular dysfunction in alzheimer disease, Nat. Rev. Neurosci. 18 (2017) 419–434.

[25] P. Lackner, R. Beer, R. Helbok, G. Broessner, K. Engelhardt, C. Brenneis, et al., Scanning electron microscopy of the neuropathology of murine cerebral malaria, Malar. J. 5 (2006) 116.
[26] A.S. Lossinsky, M.J. Song, R. Pluta, R.C. Moretz, H.M. Wisniewski, Combined conventional transmission, scanning, and high-voltage electron microscopy of the same blood vessel for the study of targeted inflammatory cells in blood-brain barrier inflammation, Microvasc. Res. 40 (1990) 427–438.
[27] A.S. Lossinsky, R. Pluta, M.J. Song, V. Badmajew, R.C. Moretz, H.M. Wisniewski, Mechanisms of inflammatory cell attachment in chronic relapsing experimental allergic encephalomyelitis: A scanning and high-voltage electron microscopic study of the injured mouse blood-brain barrier, Microvasc. Res. 41 (1991) 299–310.
[28] B.A. Maher, I.A. Ahmed, V. Karloukovski, D.A. MacLaren, P.G. Foulds, D. Allsop, et al., Magnetite pollution nanoparticles in the human brain, Proc. Natl. Acad. Sci. U. S. A. 113 (2016) 10797–10801.
[29] J. Marcus, S. Honigbaum, S. Shroff, K. Honke, J. Rosenbluth, J.L. Dupree, Sulfatide is essential for the maintenance of CNS myelin and axon structure, Glia 53 (2006) 372–381.
[30] E. Masini, L. Giannini, S. Nistri, L. Cinci, R. Mastroianni, W. Xu, et al., Ceramide: A key signaling molecule in a guinea pig model of allergic asthmatic response and airway inflammation, J. Pharmacol. Exp. Ther. 324 (2008) 548–557.
[31] L. Migliore, F. Coppede, Environmental-induced oxidative stress in neurodegenerative disorders and aging, Mutat. Res. 674 (2009) 73–84.
[32] P.V. Moulton, W. Yang, Air pollution, oxidative stress, and Alzheimer's disease, J. Environ. Public Health 2012 (2012) 472751.
[33] A. Nemmar, P.H. Hoet, B. Vanquickenborne, D. Dinsdale, M. Thomeer, M.F. Hoylaerts, et al., Passage of inhaled particles into the blood circulation in humans, Circulation 105 (2002) 411–414.
[34] G. Oberdorster, Z. Sharp, V. Atudorei, A. Elder, R. Gelein, W. Kreyling, et al., Translocation of inhaled ultrafine particles to the brain, Inhal. Toxicol. 16 (2004) 437–445.
[35] T. Okazaki, A. Bielawska, R.M. Bell, Y.A. Hannun, Role of ceramide as a lipid mediator of 1 alpha,25-dihydroxyvitamin d3-induced hl-60 cell differentiation, J. Biol. Chem. 265 (1990) 15823–15831.
[36] M. Panchal, M. Gaudin, A.N. Lazar, E. Salvati, I. Rivals, S. Ayciriex, et al., Ceramides and sphingomyelinases in senile plaques, Neurobiol. Dis. 65 (2014) 193–201.
[37] L. Peeples, News feature: How air pollution threatens brain health, Proc. Natl. Acad. Sci. U. S. A. 117 (2020) 13856–13860.
[38] R. Peters, N. Ee, J. Peters, A. Booth, I. Mudway, K.J. Anstey, Air pollution and dementia: A systematic review, J. Alzheimers Dis. 70 (2019) S145–S163.
[39] D. Pratico, Peripheral biomarkers of oxidative damage in Alzheimer's disease: the road ahead, Neurobiol. Aging 26 (2005) 581–583.
[40] E.M. Purcell, Life at low Reynolds number, Am. J. Phys. 45 (1977) 3–11.
[41] S. Rosales-Corral, D. Acuna-Castroviejo, D.X. Tan, G. Lopez-Armas, J. Cruz-Ramos, R. Munoz, et al., Accumulation of exogenous amyloid-beta peptide in hippocampal mitochondria causes their dysfunction: a protective role for melatonin, Oxid. Med. Cell. Longev. 2012 (2012) 843649.
[42] M.D. Sweeney, A.P. Sagare, B.V. Zlokovic, Blood-brain barrier breakdown in Alzheimer disease and other neurodegenerative disorders, Nat. Rev. Neurol. 14 (2018) 133–150.
[43] T. Takahashi, T. Suzuki, Role of sulfatide in normal and pathological cells and tissues, J. Lipid Res. 53 (2012) 1437–1450.
[44] J.E. Ulloth, C.A. Casiano, M. De Leon, Palmitic and stearic fatty acids induce caspase-dependent and -independent cell death in nerve growth factor differentiated pc12 cells, J. Neurochem. 84 (2003) 655–668.
[45] B.C. White, J.M. Sullivan, D.J. DeGracia, B.J. O'Neil, R.W. Neumar, L.I. Grossman, et al., Brain ischemia and reperfusion: Molecular mechanisms of neuronal injury, J. Neurol. Sci. 179 (2000) 1–33.
[46] WHO. 2020. Air pollution. Available: https://www.who.int/health-topics/air-pollution#tab=tab_1 [accessed January 23 2020].
[47] C. Wolfrum, C.M. Borrmann, T. Borchers, F. Spener, Fatty acids and hypolipidemic drugs regulate peroxisome proliferator-activated receptors alpha - and gamma-mediated gene expression via liver fatty acid binding protein: a signaling path to the nucleus, Proc. Natl. Acad. Sci. U. S. A. 98 (2001) 2323–2328.
[48] N.C. Woodward, A.L. Crow, Y. Zhang, S. Epstein, J. Hartiala, R. Johnson, et al., Exposure to nanoscale particulate matter from gestation to adulthood impairs metabolic homeostasis in mice, Sci. Rep. 9 (2019) 1816.